Structural Basis for Antagonism by Suramin of Heparin Binding to Vaccinia Complement Protein[†,‡]

Vannakambadi K. Ganesh,[§] Suresh Kumar Muthuvel,[§] Scott A. Smith,[||] Girish J. Kotwal,[||,⊥] and Krishna H. M. Murthy*[,§]

Center for Biophysical Sciences and Engineering, University of Alabama at Birmingham, Birmingham, Alabama 35294-4400, Department of Microbiology and Immunology, University of Louisville School of Medicine, Louisville, Kentucky 40202, and Division of Medical Virology and Institute for Infectious Diseases and Molecular Medicine, University of Cape Town, HSC, Cape Town, South Africa 7925

Received March 2, 2005; Revised Manuscript Received May 23, 2005

ABSTRACT: Suramin is a competitive inhibitor of heparin binding to many proteins, including viral envelope proteins, protein tyrosine phosphatases, and fibroblast growth factors (FGFs). It has been clinically evaluated as a potential therapeutic in treatment of cancers caused by unregulated angiogenesis, triggered by FGFs. Although it has shown clinical promise in treatment of several cancers, suramin has many undesirable side effects. There is currently no experimental structure that reveals the molecular interactions responsible for suramin inhibition of heparin binding, which could be of potential use in structure-assisted design of improved analogues of suramin. We report the structure of suramin, in complex with the heparin-binding site of vaccinia virus complement control protein (VCP), which interacts with heparin in a geometrically similar manner to many FGFs. The larger than anticipated flexibility of suramin manifested in this structure, and other details of VCP−suramin interactions, might provide useful structural information for interpreting interactions of suramin with many proteins.

Suramin (Figure 1) is a hexasulfonated naphthylurea that is currently being clinically evaluated in treatment of several kinds of cancer, including advanced breast cancer, nonsmall cell lung cancer (*1*), hormone refractory prostate cancer (*2*), metastatic renal cell cancer (*3*), and colorectal cancer (*4*). It is also used as an early-stage trypanocidal in treatment of trypanosomiasis (*5*). In addition, suramin has the potential to be developed as an inhibitor of herpes replication in host cells (*6*), as an inhibitor of cellular entry by flaviviridae (*7*), and as an inhibitor of protein tyrosine phosphatases (*8*). Suramin generally functions by using its negatively charged sulfonate groups to bind to basic side chains on proteins, thereby antagonizing their interaction with their natural receptors. For example, several cancers are caused by aberrant functioning of signal transduction pathways triggered by heparin-binding, angiogenic, fibroblast growth factors (*9*). Suramin is a potent inhibitor of heparin interaction with Arg and Lys residues of fibroblast growth factors (FGFs),[1] leading to its usefulness as a potential chemotherapeutic for such cancers (*10*). However, there is, currently, no available structure of suramin bound to a target protein, hampering application of structure-assisted methods in designing improved suramin analogues. Recently, crystallization and preliminary X-ray diffraction analysis of suramin complexed with a myotoxic PLA2 from *Bothrops asper* venom have been reported (*11*). Design of superior analogues acquires significant importance because suramin has several undesirable pharmacological properties, including a low therapeutic index, high metabolic stability, and toxic side effects such as anticoagulation (*12*).

We report the crystal structure of suramin, in a 1:1 complex with vaccinia virus complement control protein (VCP), at 2.2 Å resolution. VCP is the vaccinia virus homologue of the human regulators of the complement activation (RCA) family and assists the virus in evading the consequences of complement activation (*13*, *14*). It is made up of four 60 amino acid segments, termed short consensus repeats [SCRs, also called complement control protein modules (CCPs) (*15*)], each of which folds independently into a six-stranded β barrel (*16*). VCP has a heparin-binding activity that is postulated to be important for its retention in mast cells (*17*). Interaction with cell surface carbohydrates, including heparin, is of critical importance in intrinsic regulation of complement activity by regulators such as factor H (*18*). Heparin−protein interactions are also exploited by bacterial and viral mimics of host regulators in evading the host complement system (*19*). Characterization of interactions of complement regulators with heparin and heparin

[†] This research is supported by an NIH grant (AI51615) to K.H.M.M. G.J.K. is an International Senior Wellcome Trust Fellow for Biomedical Sciences in South Africa.

[‡] Atomic coordinates for the structure have been deposited in the Protein Data Bank (accession number 1Y8E).

* To whom correspondence should be addressed. Phone: 205-934-9148. Fax: 205-975-9578. E-mail: murthy@cbse.uab.edu.

[§] University of Alabama at Birmingham.

[||] University of Louisville School of Medicine.

[⊥] University of Cape Town.

[1] Abbreviations: VCP, vaccinia virus complement control protein; FGF, fibroblast growth factor; CCP, complement control protein modules; SCR, short consensus repeats; RCA, regulators of complement activation; ANS, aminonaphthalenesulfonate; NTS, naphthalenetrisulfonate.

10.1021/bi050401x CCC: $30.25
Published on Web 07/23/2005

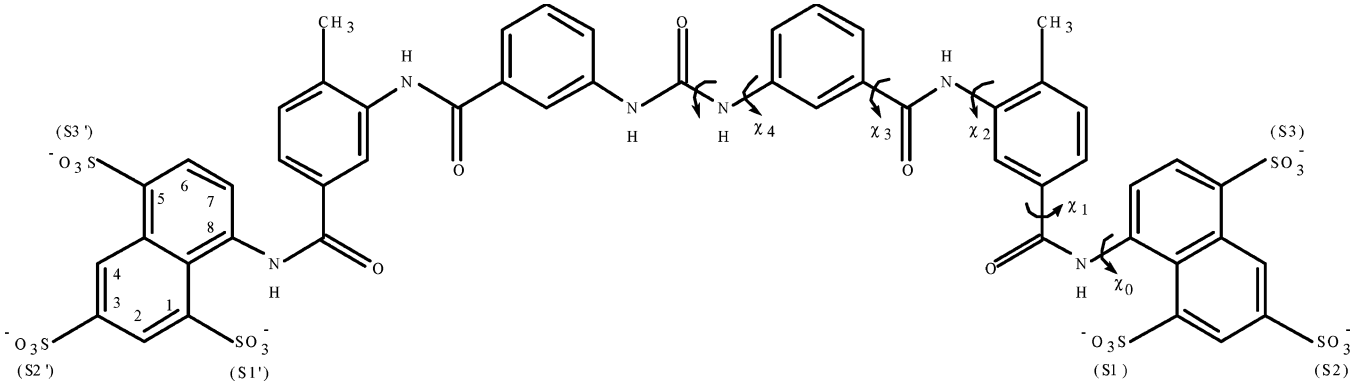

FIGURE 1: Schematic representation of suramin. Line drawing of the molecular structure of suramin. Selected atoms are labeled, and dihedral angles defining conformational freedom are marked.

antagonists is thus of significant interest in design of compounds which inhibit complement evasion by microorganisms (*20*). Experimental studies, using truncated versions of VCP, had indicated that a set of basic residues at the tip of SCR4 carried the biologically relevant heparin-binding site in VCP (*21*). VCP−heparin interaction was directly visualized by the determination of the structure of a VCP−heparin complex (*22*). VCP is functionally unrelated to fibroblast growth factors (FGFs), but its interaction with heparin is geometrically congruent to that of many heparin-binding proteins, including FGF1 (*22*, *23*). The structure of VCP−suramin is likely to provide information of potential interest to several therapeutic areas, including fibroblast growth factor antagonists, inhibitors of complement regulation, inhibitors of viral entry, and protein tyrosine phosphatase inhibitors.

EXPERIMENTAL PROCEDURES

Crystallization. Expression (*24*) and purification (*23*) of VCP have been reported. The hexasodium salt of suramin was purchased from AG Scientific, San Diego, CA. The procedure used for evaluation of suramin binding to a heparin−Sepharose column is described in the legend to Figure 2. Crystals of the complex were obtained by the vapor diffusion method at 20 °C. The reservoir solutions contained 200 mM Tris-HCl, pH 7.4, 100 mM NaCl, 2 mM $NiCl_2$, 0.2% octyl β-glucoside, and 12% PEG 3350. The 4 μL droplets, placed on cover slips, were made up from 2 μL of 600 μM VCP combined with 1.1 molar ratio of suramin, incubated at 4 °C for 30−60 min, and mixed with equal volumes of reservoir solutions. Incubations were performed in buffers containing 10 mM Tris-HCl, pH 7.4, 100 mM NaCl, and 0.02% NaN_3.

Data Measurement and Processing. Data were measured on the SERCAT beamline at the Advanced Photon Source, using a MAR CCD at 0.9791 Å. All measurements were made on flash-frozen crystals at 100 K. HKL2000 was employed for processing and scaling (*25*). Crystallographic parameters are given in Table 1.

Structure Solution and Refinement. The structure was determined through molecular replacement using BEAST (*26*) as implemented in CCP4 (*27*). The structure of native VCP (*23*) was used as the search model. The initial model for the protein was built with O (*28*) into DM (*29*) flattened maps, and the model for suramin was built into difference density. Coordinates and isotropic *B* factors were refined in CNS (*30*) using all measured data, an ML target, and a bulk solvent model. Cross-validation was performed through free *R*-values, using 10% of the reflections chosen randomly to span the resolution range; a summary is presented in Table 1. Tight noncrystallographic symmetry restraints for the two copies in the asymmetric unit were used throughout the refinement. Density for residue Cys1 is not present in either copy of VCP, and Glu108 in the second molecule (chain B) has no density for atoms Cβ and beyond. Density for OT in R244 is not present in either VCP molecule, and Pro237 in both chains adopts the cis conformation, as it does in native VCP. Solvent accessibility calculations used a 1.4 Å probe sphere. Figure 1 was made using CHEMDRAW and Figure 6 using GRASP (*31*). All other figures, except Figure 2, were made using RIBBONS (*32*). Coordinates and structure factors have been deposited at RCSB (1Y8E).

Table 1: Data Measurement and Structure Refinement

data measurement	
cell (Å; deg)	$a = 65.1$ $b = 125.1$ $c = 149.4$; $\alpha = \beta = \gamma = 90$
space group	*P*222
copies in AU	2
max resolution (Å)	2.2 (2.3−2.2)
reflections (% of possible used in refinement)	89.5 (86.5)
R_{merge} [a]	0.040 (0.113)
$\langle I/\sigma I \rangle$	18.3 (3.8)
⟨redundancy⟩	4.8 (3.2)
refinement and geometry	
R_{cryst} [a]	0.195 (0.215)
R_{free} [a]	0.249 (0.265)
bond rmsd (Å)	0.017
angle rmsd (deg)	1.4
Ramachandran outliers	0
current model	
protein atoms (⟨*B*⟩)	3709 (31.5)
suramin	172 (41.3)
water oxygen	494 (55.9)

[a] $R_{merge} = \Sigma\Sigma|I_{hi} - \langle I \rangle|/\Sigma\Sigma I_{hi}$. [b] Values for the highest resolution shell are given in parentheses.

Modeling of the FGF1−Suramin Complex. Coordinates of the crystal structure of the FGF1−heparin complex [1axm (*33*)] were used for the modeling study. Six basic amino acids at positions Lys112, Lys113, Lys118, Arg119, Arg122, and Lys128 were shown to bind heparin in the FGF1−heparin complex. The carbon atoms of Lys214, Lys220, Lys241, and Arg244 could be superimposed on corresponding atoms of Lys128, Arg122, Lys112, and Arg119 in acidic FGF with an rms deviation of 1.4 Å. The FGF1−suramin model was built by rigid body transformation of the VCP−suramin complex on FGF1.

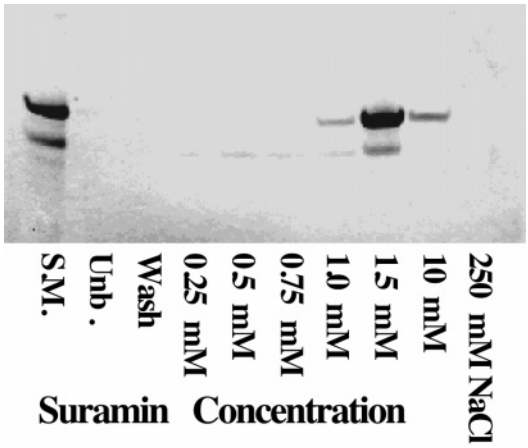

FIGURE 2: Suramin competition for heparin binding to VCP. 1.5 mg of VCP was bound to a heparin−Sepharose column in 20 mM Tris-HCl, pH 7.5, and 50 mM NaCl. The column was washed extensively with the same buffer and eluted with increasing concentrations of suramin. The eluate in each case was concentrated and run on a denaturing SDS gel.

RESULTS AND DISCUSSION

Suramin Binding by VCP and Comparison with Heparin Binding. Binding experiments using a heparin−Sepharose column indicate that suramin competes with heparin for binding to VCP (Figure 2). Although VCP has the apparent potential, based on the distribution of Lys and Arg residues in the native structure (*23*), experiments with truncated forms of the protein (*21*) and the structure of the heparin complex (*22*) have identified a single site on SCR4. Similarly, in this complex suramin interacts with the single heparin-binding site. The two copies of VCP (A and B) and suramin (C and D) in the asymmetric unit of the complex are related by a screw rotation of approximately 124°. The 243 common Cα atoms of the two VCP molecules in the complex can be superimposed with an rms deviation of 1.21 Å, and each can be superimposed onto native VCP with an rms deviation of 0.96 and 1.84 Å, respectively, for VCP-A and VCP-B for 242 Cα atoms (Figure 3). In contrast to the VCP−heparin complex, in which a hinge bending motion of SCR4 relative to SCR3 was observed, there are no significant movements of the VCP SCRs in the suramin complex (Figure 3). The suramin molecules adopt a helical conformation, with an rms deviation of 1.05 Å for all 86 atoms, between the two copies. Suramin is a highly flexible molecule due to possible free rotation about its many single bonds, including those linking the sulfonate moieties to aromatic rings (Figure 1). NMR studies and theoretical calculations have implied a molecule

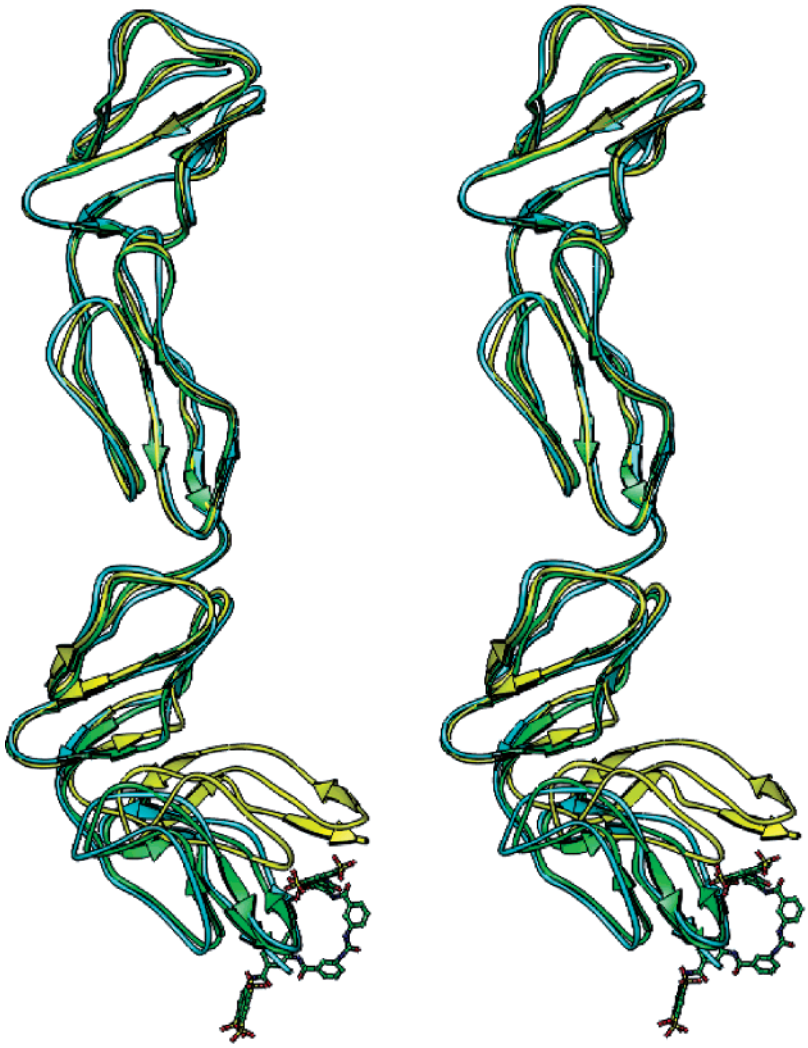

FIGURE 3: Comparison with native VCP. Superimposition of the four SCRs of VCP-B−suramin D (cyan) on those of native VCP (green). The four SCRs of VCP−heparin (yellow), using the first three SCRs for superimposition, are also shown for comparison.

with a large number of energetically accessible conformations, most of which have nonplanar arrangements of the aromatic rings around the amide linkages (*34*). Although suramin is chemically symmetric, the two halves adopt an asymmetric configuration in this structure. A rotation of 67° about the N−C bond in the urea group, and a χ_4 dihedral angle (Figure 1) of 83° in one-half of the molecule, places the two naphthalene rings on the opposite sides of the plane of the urea group. The energetically preferred configuration about the urea group in model compounds, due to steric considerations, is nonplanar, with anticipated distortions from planarity of up to 55° (*35*). The conformation of suramin is stabilized solely through interaction with VCP, as there are no suramin−suramin contacts, either within the asymmetric unit or with molecules related by crystallographic symmetry.

The interaction between VCP and suramin, like that between VCP and heparin, is dominated by electrostatic contacts, although one of the heparin ligands, Lys216, is replaced by Lys241 as a ligand to suramin. There are also small, but significant differences between the two copies of the complex in the asymmetric unit, resulting from a combination of the flexibility of both suramin and the VCP basic side chains. In VCP-B:surD, the ϵ amino groups of Lys214, Lys220, and Lys241 each form two strong hydrogen bonds (Lys214:S2′, 2.68 and 3.01 Å; Lys220:S1′, 2.74 and 2.75 Å; Lys241:S1, 2.59 and 3.16 Å) with three of the six sulfonate moieties in suramin. In addition, the guanidino group of Arg244 makes two strong hydrogen bonds (2.65 and 3.15 Å) with a fourth sulfonate group (S2) of suramin as well as a further hydrogen bond (2.88 Å) with sulfonate, S1′. Similar interactions are observed in VCP-A:surC but for Lys220 (Lys220:S1′, 2.69 Å) and Lys241 (Lys241:S1, 2.74 Å) forming one hydrogen bond respectively with sulfonate groups S1′ and S1. The conformation of the S1′ sulfonate group in surC is stabilized by two intramolecular hydrogen bonds with N1′ (2.85 and 3.09 Å) whereas, in surD, only one hydrogen bond (2.63 Å) stabilizes the S1′ sulfate group. As a result, the C−S bond connecting the naphthalene ring and sulfonate group S1′ in surC is rotated by 52°, leaving only one oxygen atom at hydrogen-bonding distance to Lys220. Due to the χ_0 angle (Figure 1) difference of about 22° in surC and surD, the sulfonate group S1 in surC is not at an optimum position to make two hydrogen bonds with Lys241 in the VCP-A−surC complex. An additional weak hydrogen bond between Tyr217 OH and sulfonate group S2′ (3.69 Å) is also observed in the VCP-A−surC complex. Additional van der Waals contacts, between VCP and suramin, in both copies are also observed. Leu221 makes van der Waals contacts with phenyl ring II (Figure 4) and sulfonate S1′. Ser222 makes contacts with phenyl ring I and Val243 with sulfonate group S1 in VCP-A−surC while Val243 in VCPB−surD makes contacts with the sulfonate group S1, phenyl ring atoms, and N2. The contacts between VCP and suramin are summarized in Figure 4. Electron density contoured around suramin atoms in the VCP-A−surC complex is shown in Figure 5A. The conformations of Lys214, Lys220, and Arg244 are significantly different from those they adopt in the heparin complex of VCP. This results, as shown in Figure 5B, in suramin spatially overlapping about half of the heparin-binding site, although three of the four basic residues that bind heparin also electrostatically contact suramin. VCP−suramin interaction buries a total of

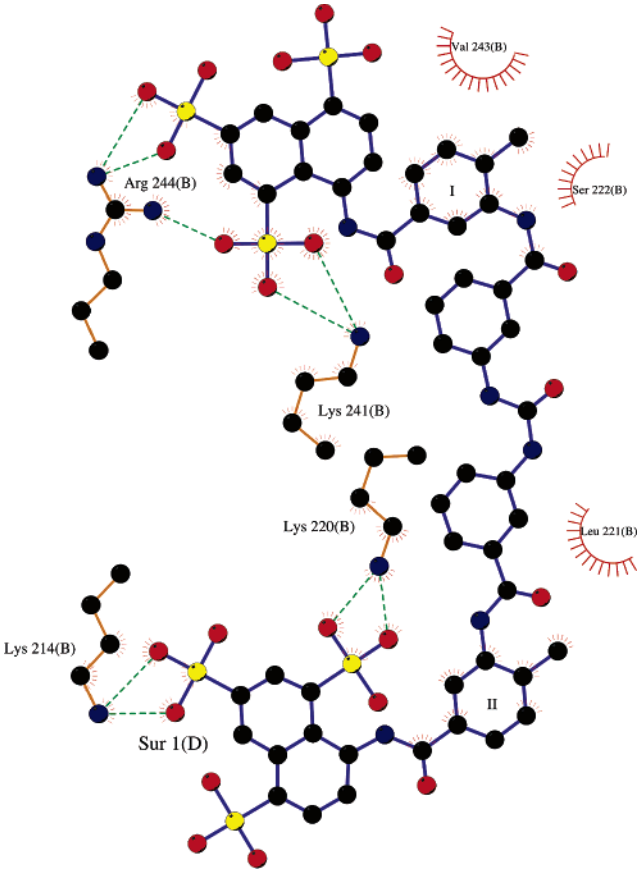

FIGURE 4: VCP−suramin contacts. Ligplot (*52*) representation of VCP-B−suramin D contacts. Suramin bonds are colored purple; protein bonds, gold. Carbon atoms are colored black, oxygen is red, nitrogen is blue, and sulfur is yellow. Hydrogen bonds are shown as dashed lines, and hydrophobic contacts are shown as semicircles with lines.

814 and 850 Å^2 of solvent-accessible surface area, respectively, in VCP-A and VCP-B. This is very similar to the average of 900 Å^2 buried in each copy of the heparin complex (*22*). The electrostatic complementarity of the positively charged SCR4 surface, and the negatively charged suramin surface, in the vicinity of their interaction is shown in Figure 6.

Implications for Suramin Binding by Other Proteins. Suramin has been widely evaluated as an inhibitor of heparin-binding fibroblast growth factors with the potential for treating a variety of cancers (*1*−*4*). The fibroblast growth factor family of proteins (FGFs 1−23) participate in many cellular events, including angiogenesis, cell migration, cell proliferation, differentiation, and morphogenesis. Although FGF11−FGF14, also known as FHF1−FHF4, possess sequence and structural homology with FGFs and bind to heparin, they fail to activate any of the seven principal FGFRs (*36*). Mechanistically, the actions of FGFs are mediated by signal transduction through fibroblast growth factor receptor (FGFR) tyrosine kinases (*9*). Formation of a ternary complex between FGF, heparin, and FGFR is a key event in this process. The stoichiometry of components in the signaling complex might be variable and depend on the nature of the components that participate. For example, a 2:2:2 stoichiometry for the FGF2:FGFR1:heparin (*37*) assembly and a 2:2:1 stoichiometry for FGF1:FGFR2:heparin assembly (*38*) in the signaling complex have been proposed.

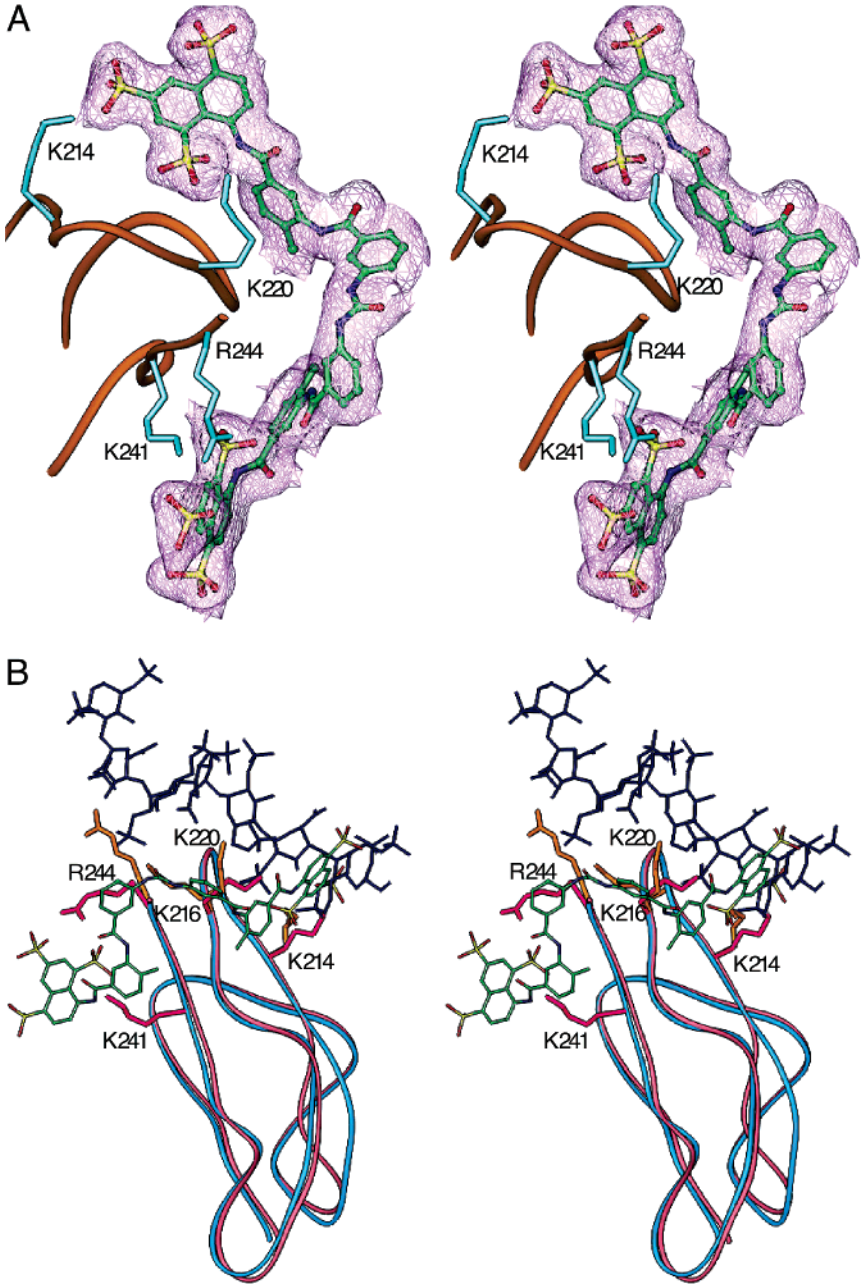

FIGURE 5: Comparison and heparin and suramin binding by VCP. (A) Segment of the $2F_o - F_c$ omit map computed using model phases and contoured around suramin C is shown, along with the corresponding atomic model. A part of the VCP-A main chain is shown as a gold ribbon. Side chains of the ligands, Lys214, Lys220, Lys241, and Arg 244, are shown as cyan stick objects. Suramin atoms are colored by atom type: carbon, green; nitrogen, blue; oxygen, red; sulfur, yellow. (B) Stereoview showing the superimposition of SCR4 of the VCP−heparin (magenta) and VCP−suramin (cyan) complex. Side chains of the ligands, Lys214, Lys216, Lys220, and Arg 244, in the VCP−heparin complex are shown as gold stick objects, and Lys214, Lys220, Lys241, and Arg 244 in VCP−suramin are shown as pink stick objects. Heparin atoms are colored blue, and suramin is colored by atom type: carbon, green; nitrogen, blue; oxygen, red; sulfur, yellow.

Recently, results from biochemical studies on the mutants of FGF and FGFR supporting the 2:2:2 stoichiometry have been reported (*39*). Nevertheless, the assembly of a dimer of the FGFR−FGF−heparin complex is a critical step in the mechanism of signal transduction initiated by FGFs, and heparin−FGF interactions are broadly similar between the models (*40*). Suramin and similar compounds are proposed to inhibit angiogenesis through prevention of the formation of heparin-mediated, physiologically productive, dimerization of FGF−FGFR−heparin by blocking the heparin-binding sites of FGF (*41*). There are currently no reported structures of suramin bound to a target protein, and in particular, obtaining the structure of a FGF−suramin complex has proved elusive (*34*, *42*, *43*). Earlier modeling studies (*23*), as well as direct comparison of structures of respective complexes, indicate that VCP−heparin interactions are geometrically similar to that between FGF1 and heparin. Although VCP and FGFs are structurally diverse proteins, the geometric positions of the heparin ligands that anchor the heparin molecule are similar and are described in a later part of the discussion. In the absence of a directly observable FGF−suramin structure, a model for suramin binding by FGFs derived through a comparison of the geometric similarities among VCP−heparin, FGF−heparin, and VCP−suramin complexes is likely to be potentially useful in design of improved analogues.

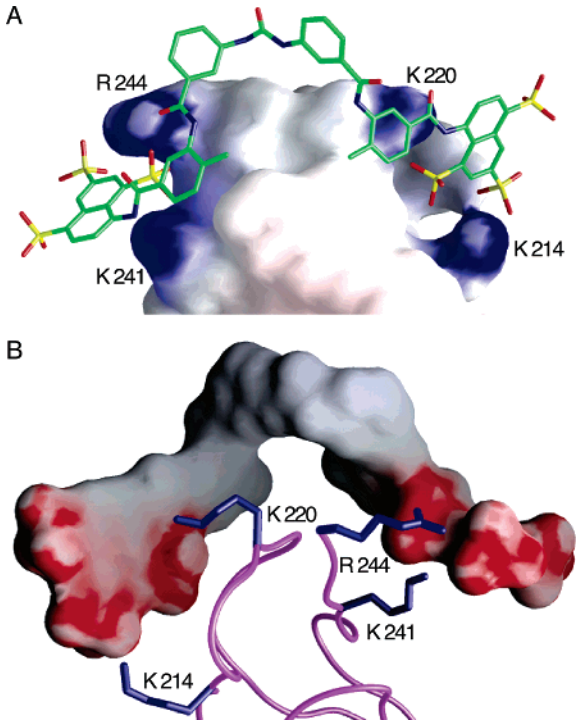

FIGURE 6: Electrostatic surfaces. (A) Electrostatic potential mapped on the molecular surface of VCP: blue, positive; red, negative. Suramin is shown as a stick object. Carbon atoms in suramin are colored green, nitrogen atoms blue, and oxygen atoms red, and sulfur is in yellow. (B) Electrostatic surface potential of suramin with portions of the VCP backbone represented as a magenta ribbon. The four basic amino acid side chains, Lys 214, Lys 220, Lys 241, and Arg244, which ligand suramin are shown as blue sticks.

The similarity of heparin interactions with FGF to that with VCP is illustrated in Figure 7A, which shows a superposition of the heparin component from several FGF−heparin complexes and the VCP−heparin complex, along with the resulting overlap of the protein components. In the heparin dodecamer−VCP complex, three lysines, 214, 216, 220, and the C-terminal Arg244 on SCR4 electrostatically tether VCP to heparin, through the latter's sulfate and carboxylate groups (*22*). The Cα atoms of the four heparin ligands, Lys214, Lys216, Lys220, and Arg244, in VCP can be superimposed over the four heparin ligands, Lys128, Arg112, Lys122, and Arg119, in FGF1 with an rms deviation of 1.1 Å. On the other hand, the Cα positions of the same four heparin ligands in FGF1 can be superimposed over the four basic residues that interact with suramin in VCP, Lys214, Lys220, Lys241, and Arg244, with an rms deviation of 1.4 Å. The latter superimposition (Figure 7B) showed no steric clashes between suramin and FGF1. In addition, after the superimposition, Lys118 in FGF1 also forms a hydrogen bond with the S1′ sulfonate group of suramin.

In the absence of an appropriate FGF−suramin structure, smaller compounds, representing substructures of suramin, have been structurally studied to gain insight into FGF−suramin interactions. Comparison of the crystallographic structure of a 5-aminonaphthalenesulfonate (ANS)−FGF1 complex (*44*) and the NMR structure of the 1,3,6-naphthalenetrisulfonate (NTS)−FGF1 complex (*45*) shows significant differences in the orientation of the naphthalene ring. Both ANS and NTS are substructures of suramin, except that the trisulfonated naphthalene ring in NTS has a sulfonate group at position 6 of the ring instead of position 5 as in suramin. Both the ANS and NTS sulfonate groups bind at the heparin site, interacting with some residues that bind heparin. Superimposition of each of the naphthalene rings in suramin, from the crystal structure, on the naphthalene rings in ANS and NTS complexes shows that suramin either has severe steric clashes with the FGF1 or no interaction is observed beyond the naphthalene ring. Therefore, an FGF−suramin model could not be readily constructed on the basis of the structural information from the ANS− and NTS−FGF complexes and experimentally determined protein-bound suramin coordinates. Although both ANS and NTS bind at a portion of the heparin-binding site, the orientations of naphthalene ring may not permit larger molecules, like suramin, to make energetically favorable contacts with FGF1. These observations suggest that while these substructures of suramin might mimic some interactions of parts of suramin, they might not be the best guides to predict the conformation that suramin itself might adopt in its complex with a given target protein. In particular, it might be somewhat challenging to synthesize larger molecules, which mimic the mode of binding adopted by suramin, through use of linkers to join substructures, as has been suggested (*48*). The structure of the VCP−suramin complex, built using the geometric similarity of the heparin-binding ligands in VCP and FGF, thus permits us to make observations that could be of significant interest to suramin interactions with FGFs and other heparin-binding proteins.

Suramin has also been shown to possess antiviral activity against enveloped viruses. An early event in infection of host cells by many viruses is attachment of the viral envelope to the heparin sulfate proteoglycans on host cell surfaces. Suramin, due to its ability to antagonize heparin binding, has been shown to inhibit this interaction. The antiviral activity of suramin has been demonstrated against herpes simplex (*6*), hepatitis C (*46*), and dengue viruses (*7*). Structures of suramin complexes with viral envelope proteins would provide the most valuable information for design of compounds to inhibit viral interactions with cell surface heparin-like molecules. However, in the absence of structures of suramin in complex with viral glycoproteins, the structure of VCP−suramin provides information, which in conjunction with structures of target proteins, such as HSV-1 glycoprotein D (*47*) and dengue virus envelope protein (*48*, *49*), would be useful in modeling studies. In particular, the small, but significant differences in VCP−suramin interactions that we observe between the two copies in the asymmetric unit strongly reinforce conclusions from earlier NMR experiments that suramin might be highly flexible (*34*). In addition, the asymmetric conformation adopted by suramin in this complex is quite different from the symmetric binding modes proposed in computational models of suramin−FGF complexes (*42*, *50*). Thus a wider range of conformations that are potentially available to suramin needs to be considered in modeling its interactions with other proteins. Finally, the nonplanarity around the urea moiety that we observe in this structure has also not been anticipated in computational models of suramin binding to other proteins (*42*, *51*) and could provide additional degrees of freedom to suramin−protein interactions. The VCP−suramin structure clearly indicates that suramin, using the flexibility available to it

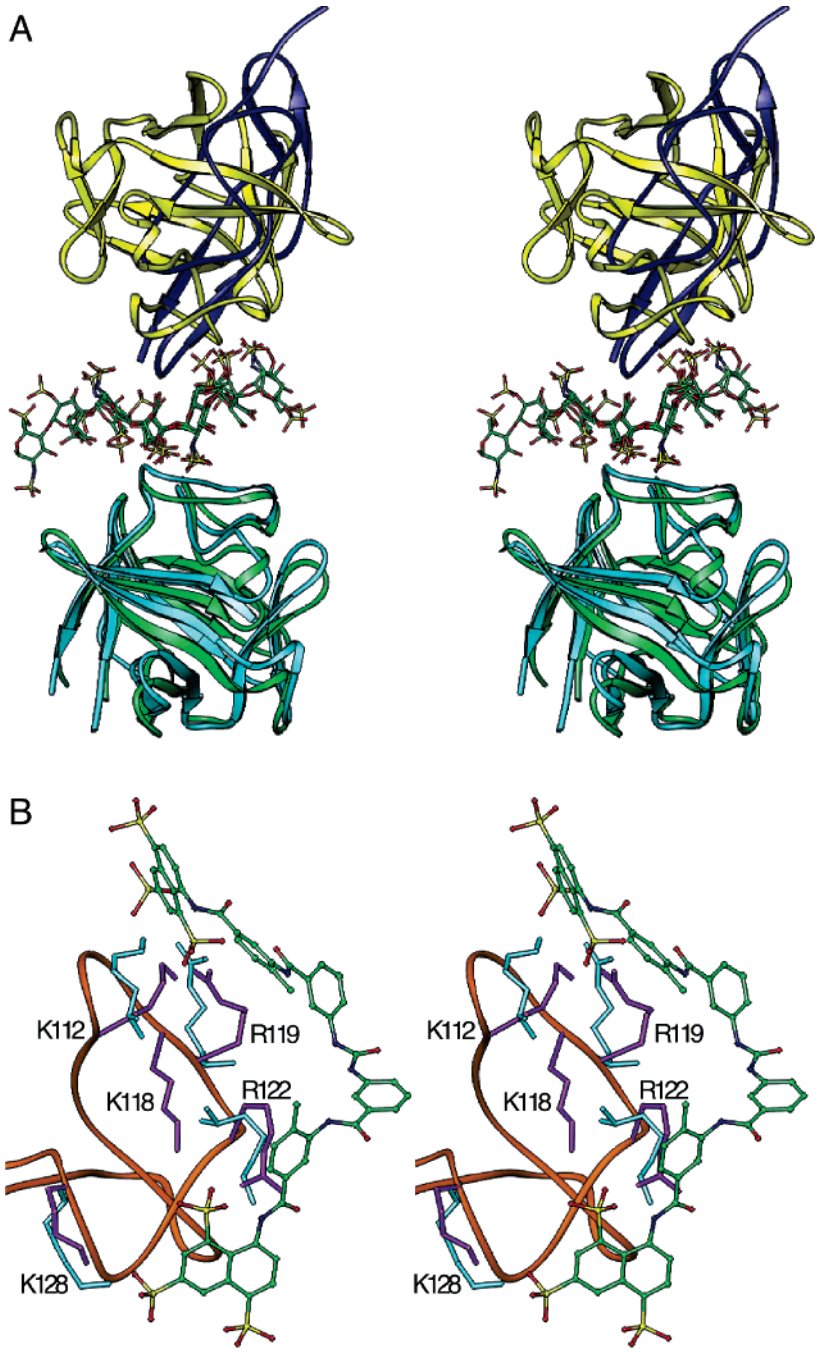

FIGURE 7: Similarity of heparin binding by FGFs and VCP and model of suramin binding to FGF1. (A) Stereoview showing carbohydrate-based superimposition of VCP, FGF1, and FGF2 complexes with heparin. VCP, FGF1, and FGF2 are represented as ribbons. VCP is colored blue, the two FGF1 molecules in the 2:1 FGF1 complex are colored green and yellow, respectively, and FGF2 is colored cyan. The three heparin molecules from the complexes are superimposed and shown as stick objects with carbon atoms colored green; nitrogen, blue; oxygens, red; and sulfur, yellow. (B) Stereoview of the modeled FGF1−suramin complex. Portions of the Cα trace of FGF1 are shown in gold. Suramin atoms are shown as ball and stick objects with carbon atoms colored green; nitrogens, blue; oxygens, red; and sulfur, yellow. The side chains of five basic residues in FGF1 are colored magenta, and the four basic residues of VCP are colored cyan. Side chain dihedral angles of FGF1 residues have been modified to orient their basic termini toward the sulfonate groups.

due to rotations about the many single bonds, adopts a conformation which maximizes the interaction with the target protein. Modeling studies on suramin interaction with other heparin-binding proteins would need to allow for such flexibility. Suitable chemical modifications imposing stereochemical restrictions might be needed to force analogues to adopt the most desirable conformation to interact with a specific target protein. Thus both the specific details of VCP interaction with suramin and the observation of conformational flexibility that we have described could be of value in designing more specific suramin analogues.

ACKNOWLEDGMENT

We thank J. Chrzas for help with data measurement at the SERCAT beamline (ID22) at APS, supported by the U.S. Department of Energy, Basic Energy Sciences. Thanks are also due to Larry DeLucas for support, to Ken Judge for

technical assistance, and to S. V. L. Narayana for previewing the manuscript.

REFERENCES

1. Mirza, M. R., Jakobsen, E., Pfeiffer, P., Lindebjerg-Clasen, B., Bergh, J., and Rose, C. (1997) Suramin in non-small cell lung cancer and advanced breast cancer. Two parallel phase II studies, *Acta Oncol. 36*, 171−174.
2. Small, E. J., Meyer, M., Marshall, M. E., Reyno, L. M., Meyers, F. J., Natale, R. B., Lenehan, P. F., Chen, L., Slichenmyer, W. J., and Eisenberger, M. (2000) Suramin therapy for patients with symptomatic hormone-refractory prostate cancer: results of a randomized phase III trial comparing suramin plus hydrocortisone to placebo plus hydrocortisone, *J. Clin. Oncol. 18*, 1440−1450.
3. Dreicer, R., Smith, D. C., Williams, R. D., and See, W. A. (1999) Phase II trial of suramin in patients with metastatic renal cell carcinoma, *Invest. New Drugs 17*, 183−186.
4. Falcone, A., Pfanner, E., Brunetti, I., Allegrini, G., Lencioni, M., Galli, C., Masi, G., Danesi, R., Antonuzzo, A., Del Tacca, M., and Conte, P. F. (1998) Suramin in combination with 5-fluorouracil (5-FU) and leucovorin (LV) in metastatic colorectal cancer patients resistant to 5-FU+LV-based chemotherapy, *Tumori 84*, 666−668.
5. Nok, A. J. (2003) Arsenicals (melarsoprol), pentamidine and suramin in the treatment of human African trypanosomiasis, *Parasitol. Res. 90*, 71−79.
6. Aguilar, J. S., Rice, M., and Wagner, E. K. (1999) The polysulfonated compound suramin blocks adsorption and lateral difusion of herpes simplex virus type-1 in vero cells, *Virology 258*, 141−151.
7. Chen, Y., Maguire, T., Hileman, R. E., Fromm, J. R., Esko, J. D., Linhardt, R. J., and Marks, R. M. (1997) Dengue virus infectivity depends on envelope protein binding to target cell heparan sulfate, *Nat. Med. 3*, 866−871.
8. Zhang, Y. L., Keng, Y. F., Zhao, Y., Wu, L., and Zhang, Z. Y. (1998) Suramin is an active site-directed, reversible, and tight-binding inhibitor of protein-tyrosine phosphatases, *J. Biol. Chem. 273*, 12281−12287.
9. Ornitz, D. M. (2000) FGFs, heparan sulfate and FGFRs: complex interactions essential for development, *Bioessays 22*, 108−112.
10. Liekens, S., De Clercq, E., and Neyts, J. (2001) Angiogenesis: regulators and clinical applications, *Biochem. Pharmacol. 61*, 253−270.
11. Murakami, M. T., Gava, L. M., Zela, S. P., Arruda, E. Z., Melo, P. A., Gutierrez, J. M., and Arni, R. K. (2004) Crystallization and preliminary X-ray diffraction analysis of suramin, a highly charged polysulfonated naphthylurea, complexed with a myotoxic-cPLA2 from *Bothrops asper* venom, *Biochim. Biophys. Acta 1703*, 83−85.
12. Kaur, M., Reed, E., Sartor, O., Dahut, W., and Figg, W. D. (2002) Suramin's development: what did we learn?, *Invest. New Drugs 20*, 209−219.
13. Kotwal, G. J., and Moss, B. (1988) Vaccinia virus encodes a secretory polypeptide structurally related to complement control proteins, *Nature 335*, 176−178.
14. Kotwal, G. J., Issacs, S. T., McKenzie, R., Frank, M. M., and Moss, B. (1990) Inhibition of the complement cascade by the major secretory protein of vaccinia virus, *Science 250*, 827−830.
15. Bork, P., Downing, A. K., Kieffer, B., and Campbell, I. D. (1995) Structure and distribution of modules in extracellular proteins, *Q. Rev. Biophys. 29*, 119−167.
16. Wiles, A. P., Shah, G., Bright, J., Perczel, A., Campbell, I. D., and Barlow, P. (1997) NMR studies of a viral protein that mimics regulators of complement activation, *J. Mol. Biol. 272*.
17. Kotwal, G. J., Reynolds, D., Keeling, K., Howard, J., and Justus, D. E. (1998) in *10th International Congress of Immunology, New Delhi, India* (Talwar, G. P., and Nath, I., Eds.) pp 315−320, Monduzzi Editore Publishing, Bologna, Italy.
18. Pangburn, M. K., Pangburn, K. L. W., Koistinen, V., Meri, S., and Sharma, A. K. (2000) Molecular mechanisms of target recognition in an innate immune system: interactions among factor H, C3b and target in the alternative pathway of human complement, *J. Immunol. 164*, 4742−4751.
19. Kotwal, G. J. (2000) Poxvirus mimicry of complement and chemokine system components: what is the end game?, *Immunol. Today 21*, 243−248.
20. Cooper, N. R. (1991) Complement evasion strategies of microorganisms, *Immunol. Today 12*, 327−331.
21. Smith, S. A., Sreenivasan, R., Krishnasamy, G., Judge, K. W., Murthy, K. H., Arjunwadkar, S. J., Pugh, D. R., and Kotwal, G. J. (2003) Mapping of regions within the vaccinia virus complement control protein involved in dose-dependent binding to key complement components and heparin using surface plasmon resonance, *Biochim. Biophys. Acta 1650*, 30−39.
22. Ganesh, V. K., Smith, S. A., Kotwal, G. J., and Murthy, K. H. (2004) Structure of vaccinia complement protein in complex with heparin and potential implications for complement regulation, *Proc. Natl. Acad. Sci. U.S.A. 101*, 8924−8929.
23. Murthy, K. H. M., Smith, S. A., Ganesh, V. K., Judge, K. W., Mullin, N., Barlow, P. N., Ogata, C. O., and Kotwal, G. J. (2001) Crystal structure of a complement control protein that regulates both pathways of complement activation and binds heparan sulfate proteoglycans, *Cell 104*, 301−311.
24. Smith, S. A., Mullin, N. P., Parkinson, J., Shchelkunov, S. N., Totmentin, A. V., Loparev, V. N., Srisatjaluk, R., Reynolds, D. N., Keeling, K. L., Justus, D. E., Barlow, P. N., and Kotwal, G. J. (2000) Surface exposed conserved K/R-X-K/R sites and positive charge on poxviral complement control proteins contribute to heparin binding and to inhibition of molecular interactions with human endothelial cells: a novel mechanism for evasion of host defense, *J. Virol. 74*, 5659−5666.
25. Otwinowski, Z., and Minor, W. (1997) in *Methods in Enzymology* (Carter, C. W., and Sweet, R. M., Eds.) pp 307−326, Academic Press, New York.
26. Read, R. J. (2001) Pushing the boundaries of molecular replacement with maximum likelihood, *Acta Crystallogr., Sect. D: Biol. Crystallogr. 57*, 1373−1382.
27. CCP4 (1993) The CCP4 suite: programs for protein crystallography, *Acta Crystallogr. D50*, 760−763.
28. Jones, T. A., Zou, J. Y., Cowans, S. W., and Kjeldgaard, M. (1991) Improved methods for building protein models in electron density and location of errors in these models, *Acta Crystallogr. A47*, 110−119.
29. Cowtan, K., and Main, P. (1998) Miscellaneous algorithms for density modification, *Acta Crystallogr., Sect. D: Biol. Crystallogr. 54* (Part 4), 487−493.
30. Brunger, A. T., Adams, P. D., Clore, G. M., DeLano, W. L., Gros, P., Grosse-Kunstleve, R. W., Jiang, J. S., Kuszewski, J., Nilges, M., Pannu, N. S., Read, R. J., Rice, L. M., Simonson, T., and Warren, G. L. (1998) Crystallography & NMR system: A new software suite for macromolecular structure determination, *Acta Crystallogr., Sect. D: Biol. Crystallogr. 54* (Part 5), 905−921.
31. Nicholls, A., Sharp, K. A., and Honig, B. (1991) Protein folding and association: insights from the interfacial and thermodynamic properties of hydrocarbons, *Proteins: Struct., Funct., Genet. 11*, 281−289.
32. Carson, M. C. (1997) in *Methods in Enzymology* (Carter, C. W., and Sweet, R. M., Eds.) pp 493−505, Elsevier Science, New York.
33. DiGabriele, A. D., Lax, I., Chen, D. I., Svahn, C. M., Jaye, M., Schlessinger, J., and Hendrickson, W. A. (1998) Structure of a Heparin-Linked Biologically Active Dimer of Fibroblast Growtf Factor, *Nature 393*, 812−817.
34. Polenova, T., Iwashita, T., Palmer, A. G., III, and McDermott, A. E. (1997) Conformation of the trypanocidal pharmaceutical suramin in its free and bound forms: transferred nuclear overhauser studies, *Biochemistry 36*, 14202−14217.
35. Dos Santos, H. F., O'Malley, P. J., and De Almeida, W. B. (1998) Gas phase and water solution conformational analysis of the herbicide diuron (DCMU): an ab initio study, *Theor. Chem. Acc. 99*, 301−311.
36. Olsen, S. K., Garbi, M., Zampieri, N., Eliseenkova, A. V., Ornitz, D. M., Goldfarb, M., and Mohammadi, M. (2003) Fibroblast growth factor (FGF) homologous share structural but not functional homology with FGFs, *J. Biol. Chem. 278*, 34226−34236.
37. Schlessinger, J., Plotnikov, A. N., Ibrahimi, O. A., Eliseenkova, A. V., Yeh, B. K., Yayon, A., Linhardt, R. J., and Mohammadi, M. (2000) Crystal structure of a ternary FGF-FGFR-heparin complex reveals a dual role for heparin in FGFR binding and dimerization, *Mol. Cell 6*, 743−750.
38. Pellegrini, L., Burke, D. F., von Delft, F., Mulloy, B., and Blundell, T. L. (2000) Crystal structure of fibroblast growth factor receptor ectodomain bound to ligand and heparin, *Nature 407*, 1029−1034.
39. Ibrahimi, O. A., Yeh, B. K., Eliseenkova, A. V., Zhang, F., Olsen, S. K., Igarashi, M., Aaronson, S. A., Linhardt, R. J., and Mohammadi, M. (2005) Analysis of mutations in fibroblast growth

factor (FGF) and a pathogenic mutation in FGF receptor (FGFR) provides direct evidence for the symmetric two-end model for FGFR dimerization, *Mol. Cell. Biol. 25*, 671−684.
40. Pellegrini, L. (2001) Role of heparan sulfate in fibroblast growth factor signalling: a structural view, *Curr. Opin. Struct. Biol. 11*, 629−634.
41. Stein, C. A. (1993) Suramin: a novel antineoplastic agent with multiple potential mechanisms of action, *Cancer Res. 53*, 2239−2248.
42. Botta, M., Manetti, F., and Corelli, F. (2000) Fibroblast growth factors and their inhibitors, *Curr. Pharm. Des. 6*, 1897−1924.
43. Middaugh, C. R., Mach, H., Burke, C. J., Volkin, D. B., Dabora, J. M., Tsai, P. K., Bruner, M. W., Ryan, J. A., and Marfia, K. E. (1992) Nature of the interaction of growth factors with suramin, *Biochemistry 31*, 9016−9024.
44. Fernandez-Tornero, C., Lozano, R. M., Redondo-Horcajo, M., Gomez, A. M., Lopez, J. C., Quesada, E., Uriel, C., Valverde, S., Cuevas, P., Romero, A., and Gimenez-Gallego, G. (2003) Leads for development of new naphthalenesulfonate derivatives with enhanced antiangiogenic activity: crystal structure of acidic fibroblast growth factor in complex with 5-amino-2-naphthalene sulfonate, *J. Biol. Chem. 278*, 21774−21781.
45. Lozano, R. M., Jimenez, M., Santoro, J., Rico, M., and Gimenez-Gallego, G. (1998) Solution structure of acidic fibroblast growth factor bound to 1,3,6-naphthalenetrisulfonate: a minimal model for the anti-tumoral action of suramins and suradistas, *J. Mol. Biol. 281*, 899−915.
46. Garson, J. A., Lubach, D., Passas, J., Whitby, K., and Grant, P. R. (1999) Suramin blocks hepatitis C binding to human hepatoma cells in vitro, *J. Med. Virol. 57*, 238−242.
47. Carfi, A., Willis, S. H., Whitbeck, J. C., Krummenacher, C., Cohen, G. H., Eisenberg, R. J., and Wiley, D. C. (2001) Herpes simplex virus glycoprotein D bound to the human receptor HveA, *Mol. Cell 8*, 169−178.
48. Modis, Y., Ogata, S., Clements, D., and Harrison, S. C. (2003) A ligand-binding pocket in the dengue virus envelope glycoprotein, *Proc. Natl. Acad. Sci. U.S.A. 100*, 6986−6991.
49. Modis, Y., Ogata, S., Clements, D., and Harrison, S. C. (2004) Structure of the dengue virus envelope protein after membrane fusion, *Nature 427*, 313−319.
50. Manetti, F., Cappello, V., Botta, M., Corelli, F., Mongelli, N., Biasoli, G., Borgia, A. L., and Ciomei, M. (1998) Synthesis and binding mode of heterocyclic analogues of suramin inhibiting the human basic fibroblast growth factor, *Bioorg. Med. Chem. 6*, 947−958.
51. Mohan, P., Hopfinger, A. J., and Baba, M. (1989) Naphthalene-disulfonic Acid derivatives as potential anti-HIV agents: chemistry, biology and molecular modeling of their inhibition of reverse transcriptase, *Antiviral Chem. Chemother. 2*, 215−222.
52. Wallace, A. C., Laskowski, R. A., and Thornton, J. M. (1995) A program to generate schematic diagrams of protein−ligand interactions, *Protein Eng. 8*, 127−134.

BI050401X